Introduction to Gaseous Detectors

Interaction Particles/Matter

Jeremie A. MERLIN

Detector lecture

Organized at University of Seoul, Seoul

January, 2024

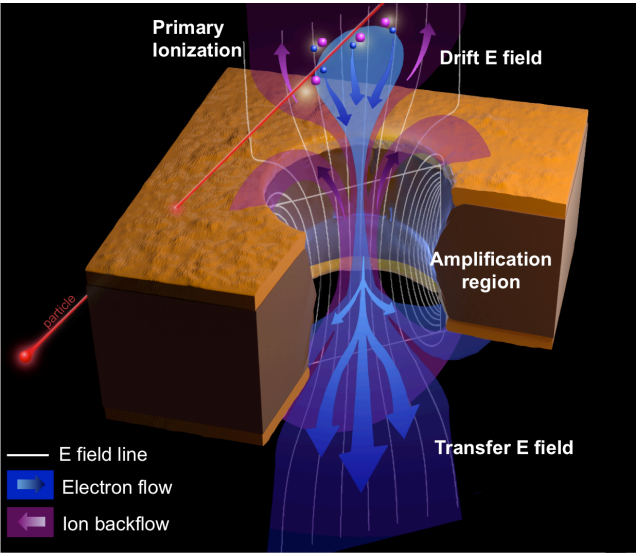

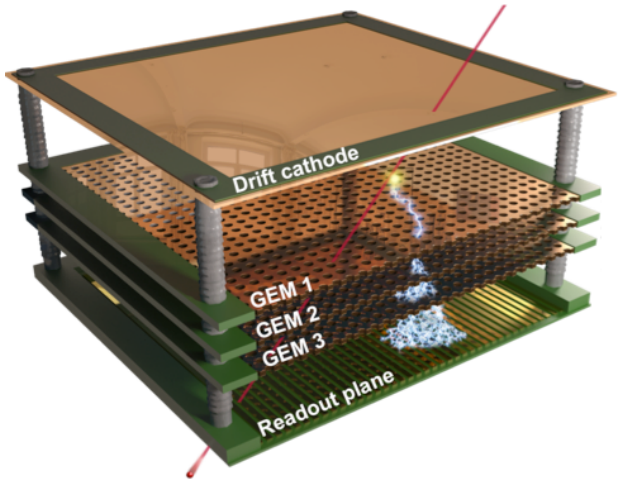

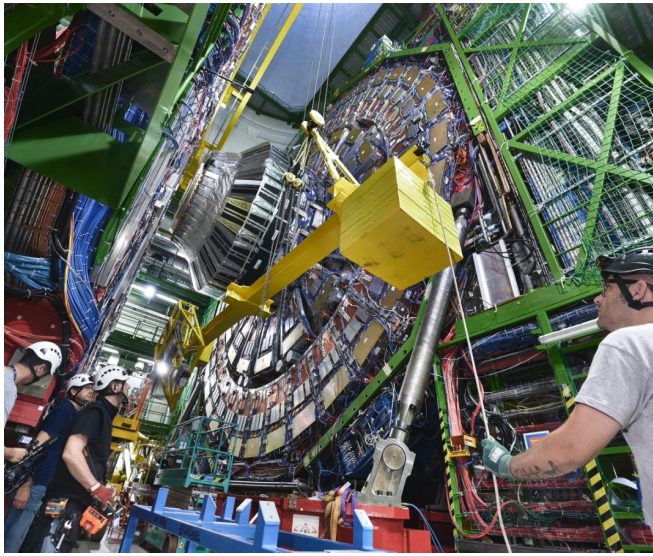

Introducing Myself

Jeremie A. Merlin
Particle Physicist
Specialized in Detector Physics

- I joined the CMS GEM upgrade project in 2011
- My main responsibility is the coordinate the development of the triple-GEM technology for the CMS upgrade and to manage the production and quality control of the detectors

Contact:
Jeremie.alexandre.merlin@cern.ch

Education

Apr. 2016	**Ph.D in Particle Physics**, University of Strasbourg Thesis: "Study of the long-term sustained operation of gaseous detectors for the high rate environment in CMS" *Conducted at CERN under the supervision of Archana Sharma (CERN) and Jean-Marie Brom (Institut Pluridisciplinaire Hubert Curien - IPHC Strasbourg)*
Sep. 2012	**Master in Engineering Sciences and Applied Physics**, Telecom Physique Strasbourg (TPS) Project: "Development of a DAQ prototype for the analysis and the reconstruction of fingerprints on bullet casings for the french national police"
Jul. 2012	**Master in Subatomic and Astroparticle Physics**, University of Strasbourg Thesis: "Study of the aging processes in GEM detectors for CMS" *Conducted at CERN under the supervision of Archana Sharma (CERN)*

Responsibilities

Current Sep. 2019	**GEM Phase II Detector R&D Coordinator** *My role is to coordinate the different activities regarding the development of the triple-GEM technology for the CMS application: Optimisation of the detector configuration; Longevity studies; Discharge and crosstalk mitigation; Rate capability optimisation. I am continuously monitoring the progress on the different fronts of developments, I provide technical expertise, define the main timeline and the milestones.*
Current Sep. 2019	**GE2/1 Detector Production Coordinator** *My role is to coordinate the assembly, the quality control and the validation of 300 GE2/1 detectors in various production sites distributed all around the world. Specifically, I provide technical expertise, guidelines and I define the main production schedule and milestones.*
Feb. 2021 Sep. 2017	**GE1/1 Detector Production Coordinator** *My role was to coordinate the assembly, the quality control and the validation of 144 GE1/1 detectors in various production sites distributed all around the world. Specifically, I provided technical expertise, guidelines and I defined the main production schedule and milestones. All the chambers and the spares were successfully produced, tested and delivered in time for the installation in CMS.*
Current Jun. 2016	**CMS Safety Officer** *Deputy Flammable Gas Safety Officer (FGSO). In charge of the safety related to the use of flammable gas in the CMS experiment.*
Current Jan. 2017	**GEM Laboratory Manager** *Responsible for organising the activities in the central GEM production laboratory at CERN. It includes the preparation of the test stands, the management of the safety, the coordination of the various R&D activities and the supervision of the workers and students.*

Introduction

Simplified view

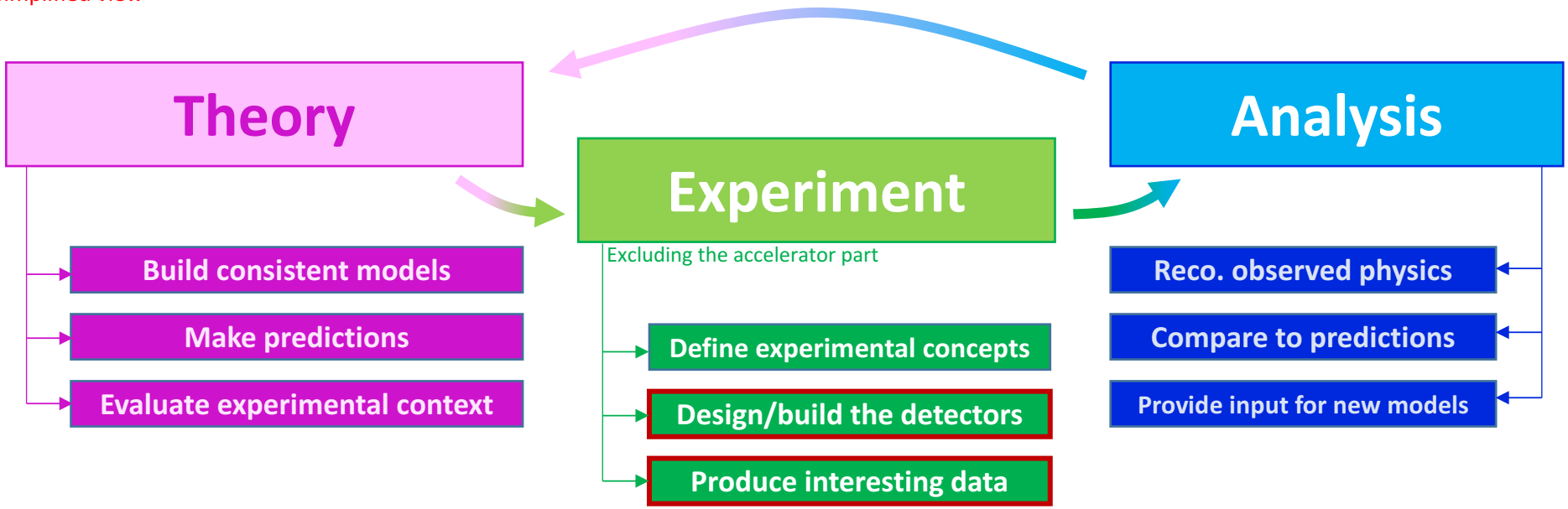

- **Experimental physics - Detector physics**

- What is the final purpose ? → Detect particles
- **How to detect particle ? → Based on the particle/matter interaction processes**
- How to design and build detectors ? → various options
- (- How to install and operate detectors)

- **Lets see the cases of:**

- Charged particles
- Photons
- Neutrons

Charged Particles

A fast charged particle traversing a medium will interact with it via EM, weak or strong forces. However, the weak interaction is by definition negligible for most of the particles (except neutrinos) and the typical range of the strong interaction is at the order of the nuclear section, i.e. 10^8 to 10^{10} orders of magnitude lower than the atomic section. The EM interaction is thus the predominant process for the detection of charged particles. The highest probable process within the EM interactions is the Coulomb interaction between the EM fields of the particle and of the medium. It leads to the excitation and/or the ionization of the medium itself, resulting in the release of free charges that can be used to generate electronics signals.

Energy loss due to Coulomb interactions

The average energy lost by a particle passing through a material is given by the Bethe-Bloch formula:

$$-\left\langle \frac{dE}{dx} \right\rangle = \frac{2\pi e^4 z^2}{m_e c^2 \beta^2} NZ \left[ln\left(\frac{2m_e c^2 \beta^2 \gamma^2 T_m}{I^2} \right) - 2\beta^2 - \delta(\beta\gamma) \right] \tag{4.1}$$

where ze is the charge of the incoming particle, m_e the mass of the electron at rest, N and Z the atomic density and atomic number of the medium. The parameter I represents the average ionization and excitation potential of the medium. The maximum energy transfer for a single interaction is represented by the parameter T_m given by:

$$T_m = \frac{2m_e c^2 \beta^2}{1 - \beta^2} \tag{4.2}$$

Energy loss due to Coulomb interactions

The validity of the Bethe-Bloch formula in this form is limited to $0.1 \lessapprox \beta\gamma \lessapprox 1000$. For $\beta\gamma \gtrapprox 4$ we observe a relativistic rise of the stopping power due to the increase of the transverse electric field of the particle and therefore the increase of distant interaction contributions. However, the polarization of the medium limits the field extension and acts as a shielding of the electrical field far from the particle path, cutting the long-range contributions. The Fermi density effect correction $\delta(\beta\gamma)$ is introduced in Equ. (4.1) to cover this phenomenon. At very low energies ($\beta\gamma \lessapprox 0.1$), the assumption that the electron is at rest is no longer valid. The particle velocity is comparable to the orbital velocity of the atomic electrons, which allows electron capture processes. Additional corrections such as shell corrections, Bloch correction and Barkas correction are required to fully describe the low energy range. At higher energies ($\beta\gamma \gtrapprox 10^4$ for muons), radiative processes become more important than ionization. The average energy loss $\left\langle \frac{dE}{dx} \right\rangle$ is no longer a continuous function of the parameter $\beta\gamma$, based on Coulombs interactions, but a complex combination of various effects such as e^+e^- pair production, Bremsstrahlung and photo-nuclear interactions.

Energy loss due to Coulomb interactions

In the case of the HEP experiments, and particularly the CMS muon system, most of the relativistic particles have a mean energy loss close to the minimum, they are identified as "Minimum Ionizing Particles" (MIP). An example of the average energy loss of a positive muon in copper is shown on Fig. 4.1.

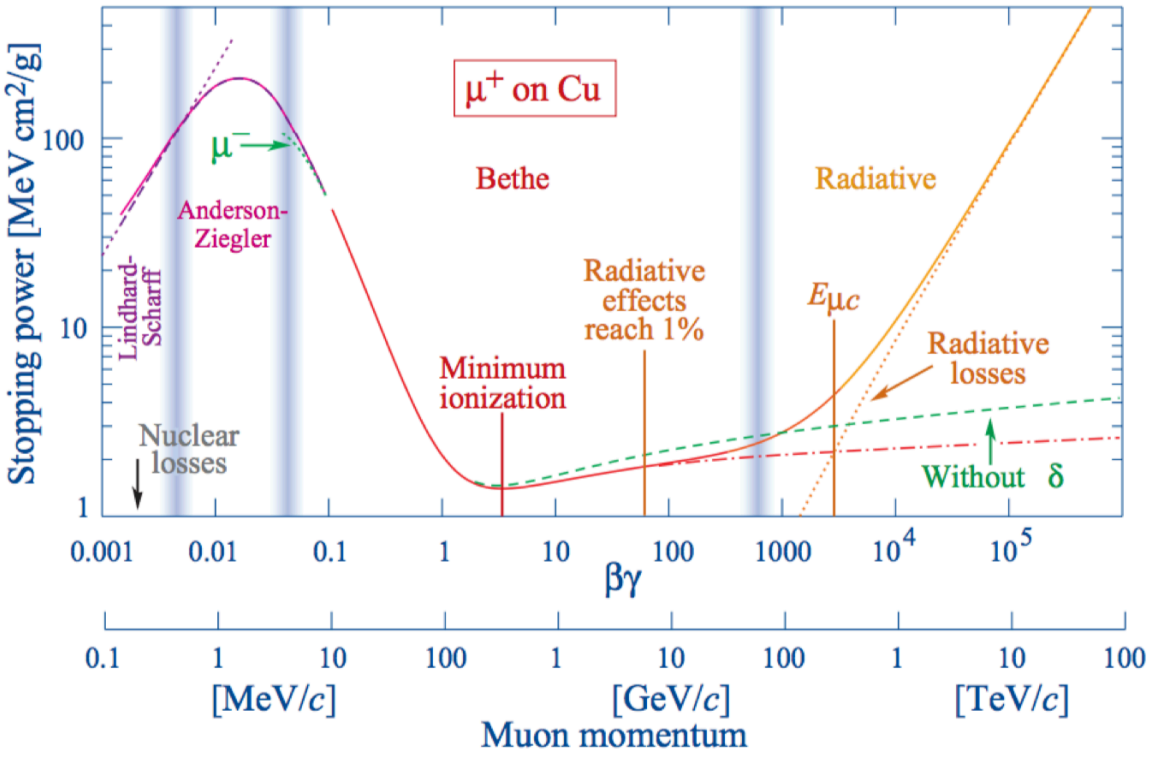

FIGURE 4.1: Stopping power for positive muons in copper as a function of $\beta\gamma$.

Energy loss due to Coulomb interactions

The CMS muon detectors essentially operate in argon-based mixtures. As indicated on Fig. 4.2, the average energy loss of MIPs in argon is close to 1.53 MeV g^{-1} cm^2. Considering the density of argon $\rho = 1.78 \times 10^{-3}$ g cm^{-3}, the total energy loss per unit length in pure argon becomes:

$$\Delta E_{argon} = -\left\langle \frac{dE}{dx} \right\rangle \times \rho \times d = 1.53 \times 1.78 \times 10^{-3} \times 1 = 2.72\ keV/cm \qquad (4.3)$$

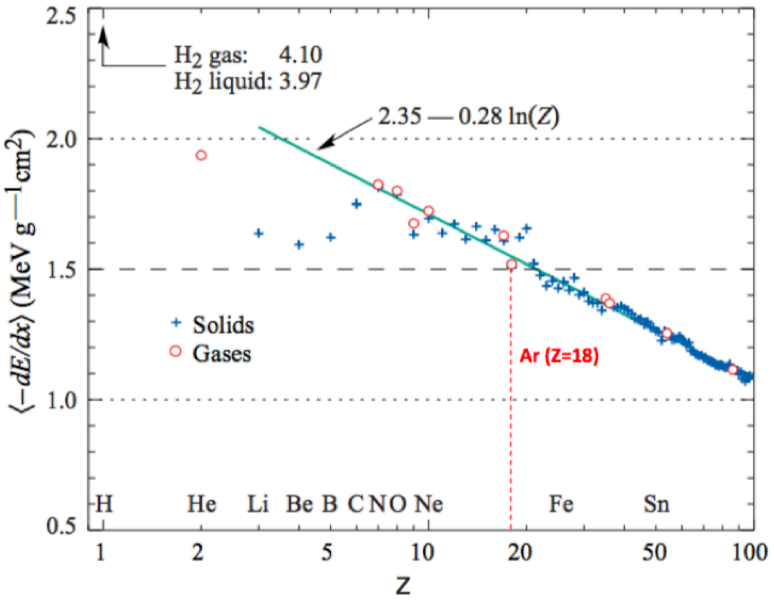

FIGURE 4.2: Energy loss of a MIP as a function of the atomic number of the medium

Energy loss fluctuations

The energy loss described in the previous section is an average value. Since it involves collisions with atoms, which are subject to statistical fluctuations, the energy loss and the electron-ion pair production for a given path length are also subject to fluctuations. Similarly, for a given energy loss value, the path length before the particle is stopped, or range of the particle, fluctuates. This phenomenon is called straggling and leads to the widening of the energy loss distribution of a particle passing through a medium, especially on the side of the high energy losses. In the case of a thin layer of absorber, the energy loss distribution is described by the Landau-Vavilov expression:

$$f_{L,V}(\Delta, \beta\gamma, x) = \phi(\lambda) = \frac{1}{\sqrt{2\pi}} e^{-\frac{1}{2}(\lambda + e^{-\lambda})} \qquad (4.4)$$

where x is the thickness of the medium. The energy variable λ represents the deviation between the specific case energy loss Δ/x and the most probable energy loss Δ_p/x:

$$\Delta_p/x = \xi \left[ln\frac{2m_e c^2 \beta^2 \gamma^2}{I} + ln\frac{\xi}{I} + 0.2 - \beta^2 - \delta(\beta\gamma) \right] \qquad (4.6) \qquad \xi = \frac{2\pi e^4 z^2}{m_e c^2 \beta^2} NZx$$

Energy loss fluctuations

Example

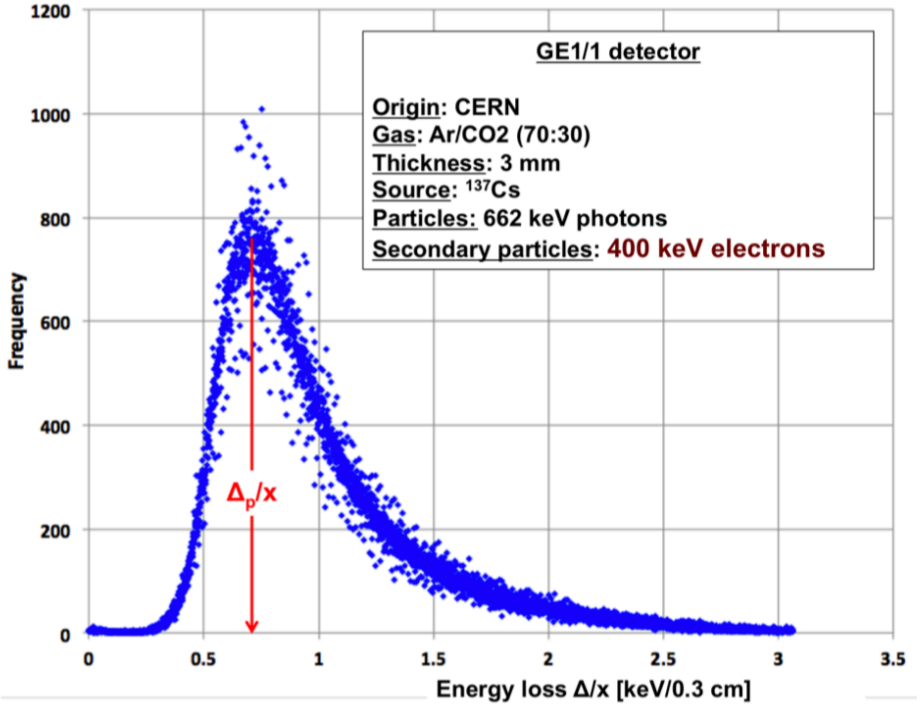

FIGURE 4.3: Energy distribution of $\sim$ 400 keV electrons in a gaseous detector operating in Ar/CO_2 (70 : 30). The electrons are produced from the Compton interaction of 662 keV photons with copper in front of the gas volume.

Ionization Process

In the case the energy is lost by ionization, the incoming particle liberates a discrete number of electron-positive ion pairs in the medium. This process is called primary ionization. The freed electron may possess sufficient kinetic energy to cause secondary ionization events in the medium. Such electrons are sometimes called δ-rays and their number n per unit length dx for a kinetic energy between T and dT can be estimated by:

$$\frac{d^2n}{dTdx} = \frac{2\pi z^2 e^4}{m_e c^2 \beta^2} NZ \frac{1}{T^2} \left[1 - \beta^2 \frac{T}{T_m}\right] \tag{4.8}$$

where ze is the charge of the incoming particle, m_e the mass of the electron at rest and N and Z the atomic density and atomic number of the medium. The maximum energy that can be transferred to the electron by a massive particle is given by

$$T_m = 2m_e c^2 \beta^2 \gamma^2 \tag{4.9}$$

Ionization Process

The total number of electron-positive ion pairs in a given volume produced by both primary and secondary ionization can be expressed by:

$$n_T = \frac{\Delta E}{W_i} \tag{4.10}$$

where ΔE is the total energy loss transferred to the given volume and W_i is the effective average energy to produce one electron-positive ion pair. The parameter W_i is usually bigger than the average ionization and excitation potential I (Equ. (4.1)) since a fraction of the deposited energy is absorbed by excitation processes and doesn't necessarily release electrons in the medium.

Ionization Process

Example

If the target medium contains several components, the average energy W_i of the medium is calculated following a simple composition law. For example, we can calculate the total number of primary electrons produced by MIPs in a muon detector operating in Ar/CO_2 (70 : 30). Following the same procedure as for Equ. (4.3), the total energy loss transferred to the medium over a distance of 3 mm (typical conversion length for a GE1/1 detector) is $\Delta E = 861$ eV. Therefore:

$$n_T = \Delta E \left[\frac{0.7}{W_i(Ar)} + \frac{0.3}{W_i(CO_2)} \right] = 861 \left[\frac{0.7}{26} + \frac{0.3}{33} \right] \approx 31 \; pairs \qquad (4.11)$$

Photons

The photons also interact via electromagnetic effects. But while a charged particle shows a continuous energy loss in the medium, the absorption of a photon is a single localized event. Considering a beam of photons with the energy E and an intensity I crossing a medium with a thickness x, the intensity loss is given by:

$$dI = -N\sigma(E, Z)I dx \tag{4.12}$$

where σ is the total cross-section of the interaction for a given material with an atomic number Z and an atomic density N. If the initial intensity of the beam is I_0, the total attenuation is:

$$\frac{I}{I_0} = e^{-N\sigma(E,Z)x} = e^{-(\mu/\rho)X} \tag{4.13}$$

where $(\mu/\rho) = N(\sigma/\rho)$ is, by definition, the mass attenuation coefficient, $X = \rho x$ is the reduced thickness of the medium and ρ the density of the medium.

Absorption Mechanisms

There are several mechanisms of absorption with different relative importances depending on the energy of the photons, as shown in Fig. 4.4. At energies lower than several 10 keV, the dominant process is the photoelectric absorption; then the Compton scattering (or incoherent scattering) up to several tens of MeV; at higher energies, the dominant process is the electron-positron pair production. The total attenuation coefficient is simply defined as the sum of all the partial coefficients:

$$\left(\frac{\mu}{\rho}\right)_{total} = \left(\frac{\mu}{\rho}\right)_{photoelectric} + \left(\frac{\mu}{\rho}\right)_{Compton} + \left(\frac{\mu}{\rho}\right)_{pair}$$

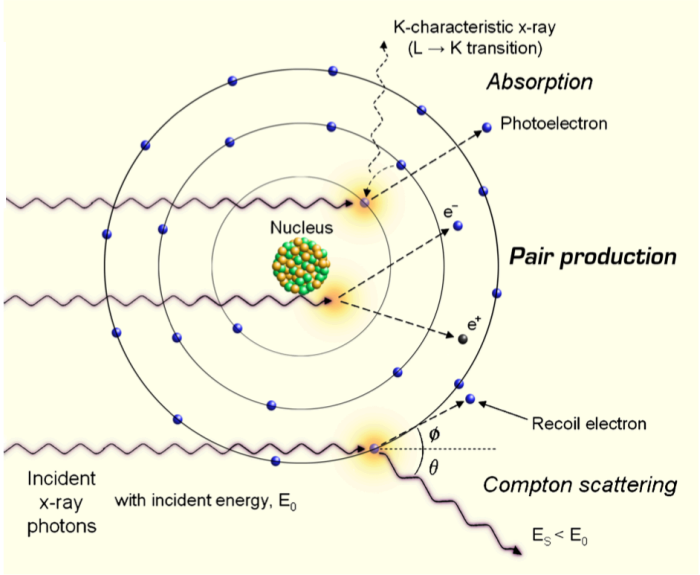

FIGURE 4.4: The main absorption processes of the photon interaction.

Absorption Mechanisms Example

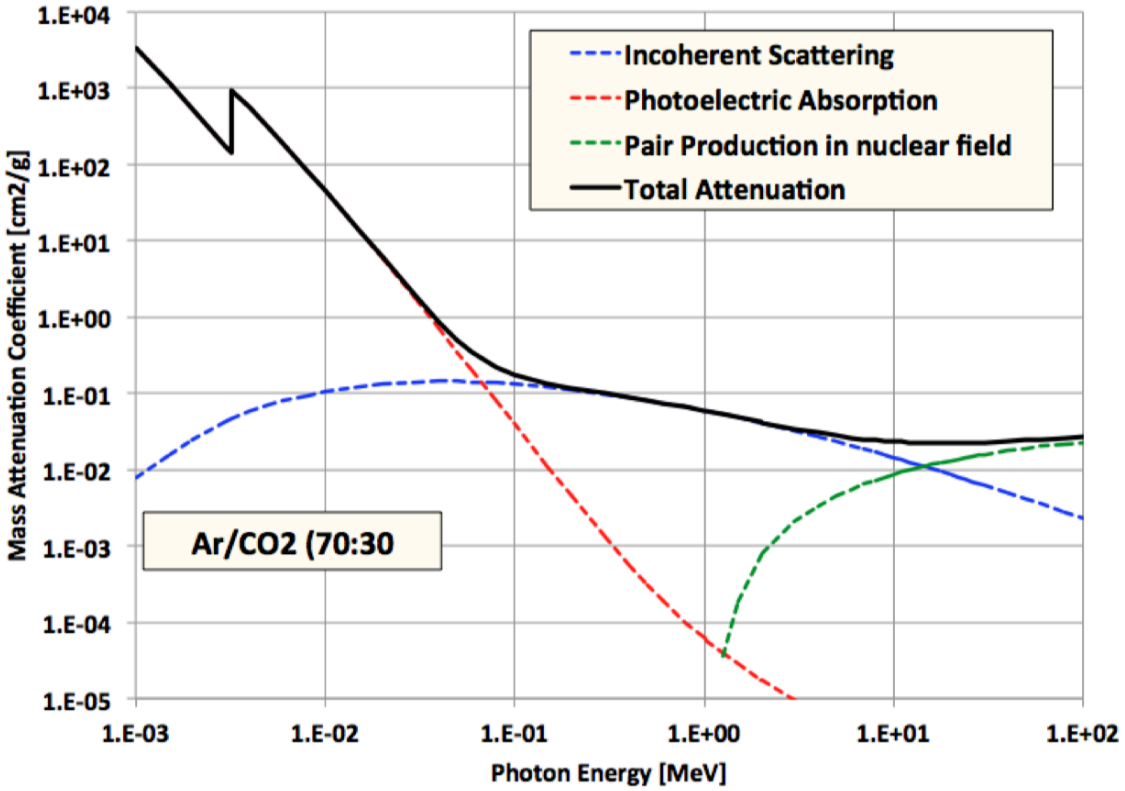

FIGURE 4.5: Total and partial mass attenuation coefficients in Ar/CO_2 (70 : 30)

Each of these processes is complex and accompanied with secondary effects such as fluorescent radiations, emission of Auger electrons, recoil electrons or annihilation of positrons.

Photo-electric Effect

In the case of photoelectric absorption, the total energy of the incoming photon is spent to remove one electron from an inner shell of the atom. This process is possible only if the energy E_γ of the photon is higher than the binding energy E_j of the electron to be removed. All the levels having $E_j \leq E_\gamma$ contributes to the photoelectric absorption. The effect is maximum at the edge and then decreases with the energy, giving a series of characteristic jumps in the absorption coefficient as seen in Fig. 4.5. The electron ejected from the atom has an energy $E_e = E_\gamma - E_j$ and leaves the medium in an excited state. The medium then returns to its ground state through two competing mechanisms:

- The first possibility, called Auger process, corresponds to an internal electronic rearrangement and the emission of an electron. For example, a vacancy in the K-shell may be filled by an electron from the L-shell which gives its energy to a M-shell electron that is ejected from the atom. This electron is called Auger electron and its kinetic energy is given by:

$$E_{Auger} = E_K - E_L - E_M \tag{4.15}$$

Photo-electric Effect

- In the second process called fluorescence, the vacancy on a j-shell is filled by an electron from a outer i-shell by emitting an X-ray photon with an energy $E_{Xray} = E_j - E_i$ where E_j and E_i are respectively the binding energies of the j-shell and the i-shell. The fraction of de-excitation by fluorescence, called fluorescence yield, is shown for the shells K and L on Fig. 4.6.

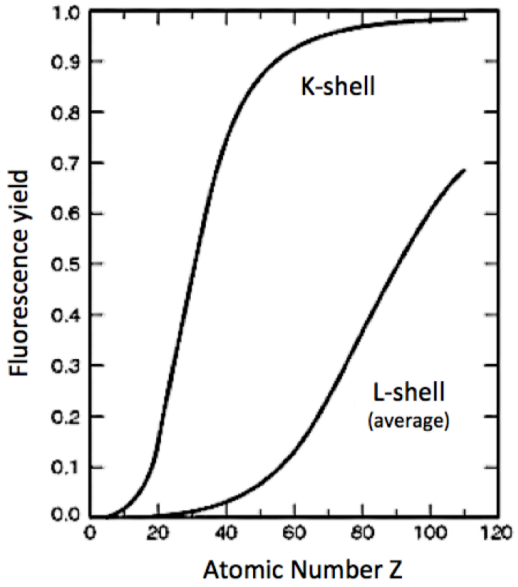

FIGURE 4.6: Fluorescence yields for K and L shells as a function of the atomic number Z. The curve for the L-shell is an average of L_1,L_2 and L_3 effective yields.

Compton Scattering

The photoelectric absorption cross-section falls very quickly after the K-edge, as shown in Fig. 4.5. At energies above the highest atomic level, the intensity loss of a photon beam is dominated by the elastic incoherent scattering on nearly free electrons of the medium, also called the Compton scattering. When an incident photon is scattered an angle θ, the electron recoils with an angle ϕ as shown on Fig. 4.4. The energy $E_{\gamma'}$ of the scattered photon and the energy E_e of the recoil electron are given by:

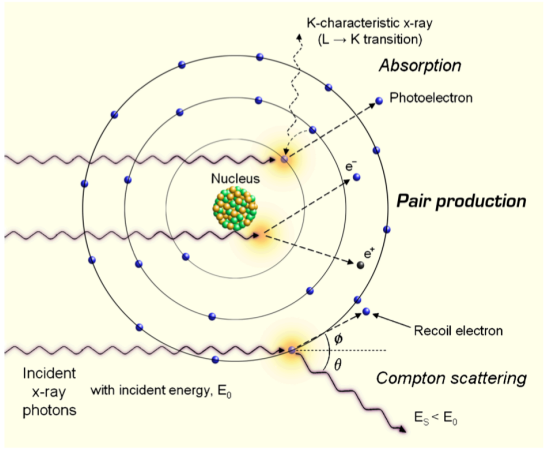

$$E_{\gamma'} = \frac{E_\gamma}{1 + \varepsilon(1 - cos\ \theta)} \tag{4.16}$$

with $\varepsilon = E_\gamma / m_e$.

$$E_e = \frac{E_\gamma \varepsilon (1 - cos\ \theta)}{1 + \varepsilon(1 - cos\ \theta)} \tag{4.17}$$

FIGURE 4.4: The main absorption processes of the photon interaction.

Compton Scattering

In the case of back scattering (i.e $\theta = \pi$), the electron obtains the maximum energy:

$$E_e^{max} = \frac{E_\gamma}{1 + \frac{1}{2\varepsilon}} \tag{4.18}$$

Fig. 4.7 shows the energy distribution of the recoil electrons for different incident photon energies. The maximum energy, corresponding to the back scattering event is known as the Compton edge.

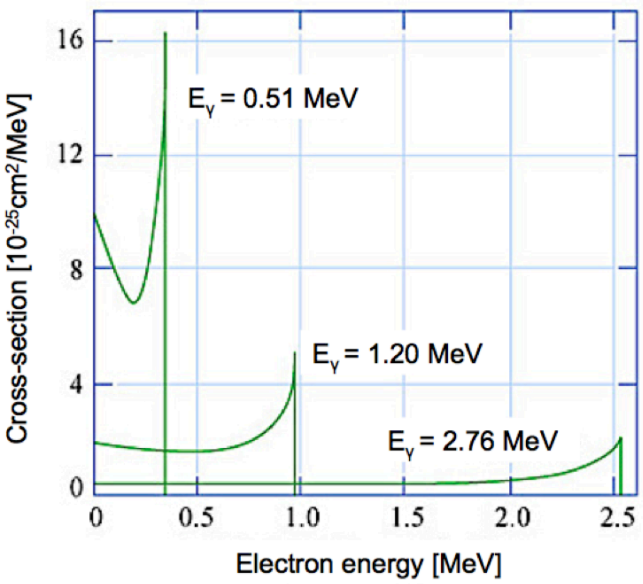

FIGURE 4.7: Energy distribution of Compton electrons for several incident photon energies.

Compton Scattering

The emission angle of the recoil electron is given by:

$$cot(\phi) = (1 + \varepsilon)\ tan\ \theta/2 \tag{4.19}$$

At low energies (i.e $\varepsilon << 1$), the scattering cross-section for a single electron can be reduced to:

$$\sigma_c^e = \sigma_{Th}^e(1 - \varepsilon) \quad with \quad \sigma_{Th}^e = \frac{8}{3}\pi r_e^2 \tag{4.20}$$

Where σ_{Th}^e is the Thomson cross-section and r_e the electron radius. At high energies (i.e $\varepsilon >> 1$), the cross-section is:

$$\sigma_c^e = \frac{\pi r_e^2}{\varepsilon}(\frac{1}{2} - ln(2\varepsilon)) \tag{4.21}$$

Compton Scattering

The total differential cross-section for a solid angle Ω is given by the Klein-Nishina angular distribution:

$$\frac{d\sigma_c^e}{d\Omega}(\theta) = r_e^2 \left(\frac{1}{1+\varepsilon(1-cos\ \theta)}\right)^2 \left(\frac{1+cos^2\ \theta}{2}\right) \left(1+\frac{\varepsilon^2(1-cos\ \theta)^2}{(1+cos^2\ \theta)(1+\varepsilon(1-cos\ \theta))}\right) \tag{4.22}$$

The atomic cross-section is:

$$\sigma_c^{atom} = Z\sigma_c^e \tag{4.23}$$

where Z is the atomic number of the medium. The angular distribution as a function of the incident energy and the polar diagram of the total cross-section are shown in Fig. 4.8 and Fig. 4.9.

Compton Scattering

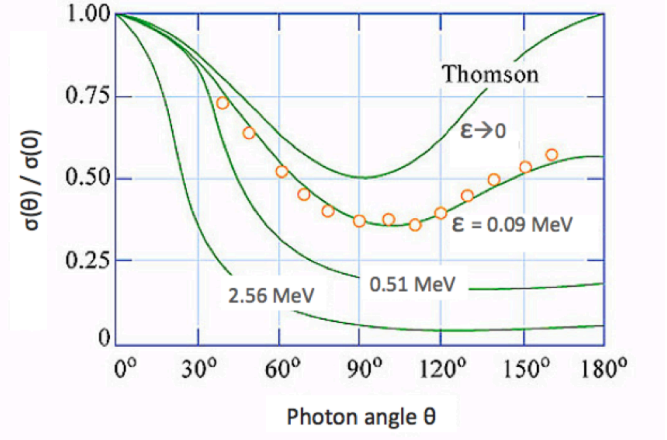

FIGURE 4.8: Angular distribution of scattered photons for several incident energies ε.

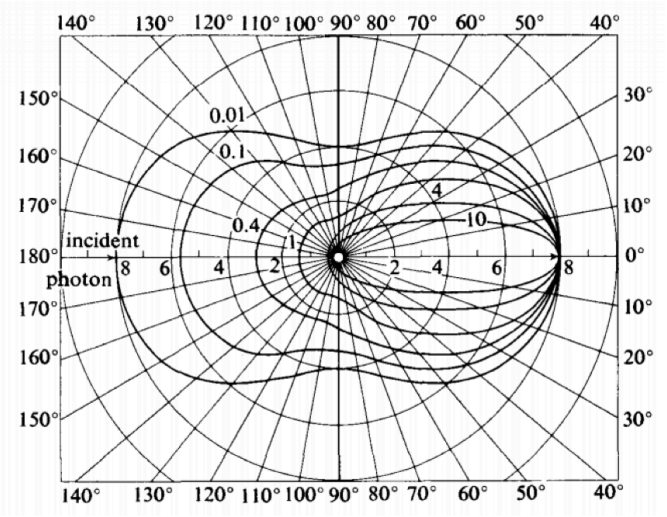

FIGURE 4.9: Polar diagram of the differential Compton cross-section per electron. Curves labeling corresponds to the incident photon energy ε. $d\sigma/d\Omega$ is expressed in $\mathrm{cm}^2\ \mathrm{sr}^{-1}$

Electron-Positron Pair Production

During the pair production, or materialization, the photon is absorbed by producing an electron-positron pair in the medium. This is the dominant process of interaction at high energies and requires the presence of a nucleus or an electron to balance the momentum conservation during the transformation.

A particle at rest has a minimum energy $E^2 = m_0^2 c^4$ with negative and positive solutions. The region between these solutions corresponds to the forbidden energies, as shown in Fig. 4.10.

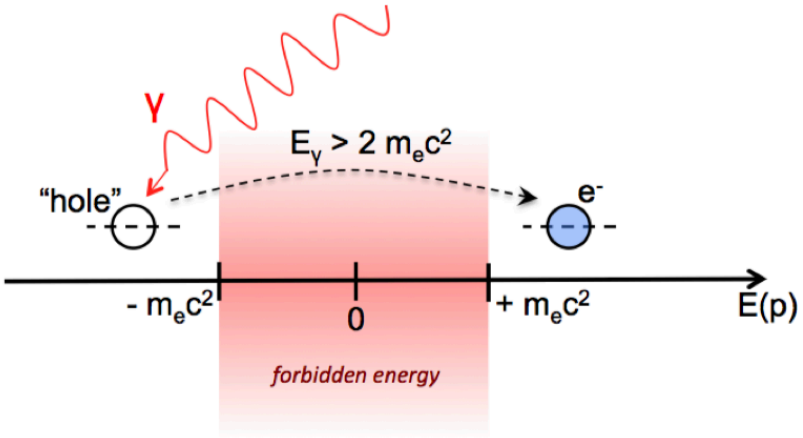

FIGURE 4.10: Schematic view of the Dirac sea in the case of an electron-positron pair production.

Electron-Positron Pair Production

The materialization energy is used to bring a particle from a negative energy state, also called the Dirac sea, to the positive domain. A "hole" is then left in the Dirac sea corresponding to an anti-matter particle. In the case of an electron-positron pair produced by a photon crossing the electric field of a nucleus, the threshold energy is $2m_ec^2 = 1.022$ MeV. The positron has a high probability to be annihilated in the medium, producing one or several energetic photons. If the secondary photons have an energy higher than the threshold energy, they will trigger more materialization and annihilation processes and create an electromagnetic shower in the medium.

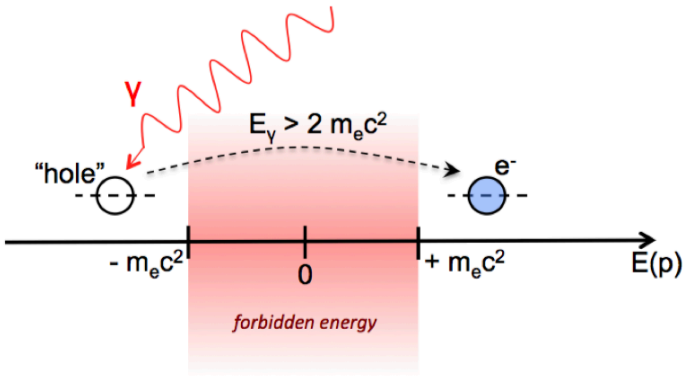

FIGURE 4.10: Schematic view of the Dirac sea in the case of an electron-positron pair production.

Neutrons

Since neutrons are uncharged particles, they are not sensitive to Coulomb interactions with the medium but they can provoke collisions with the atoms or interact directly with the nuclei via nuclear reactions. Therefore it is very difficult to detect free neutrons, especially with gaseous detectors. However, a neutron passing through a detector can interact with the material surrounding the gas volume and produce secondary emission of charged particles or photons that may ionize or excite the gas. We can identify five main interactions with different probabilities depending on the neutron incident energy, as shown on Fig. 4.11.

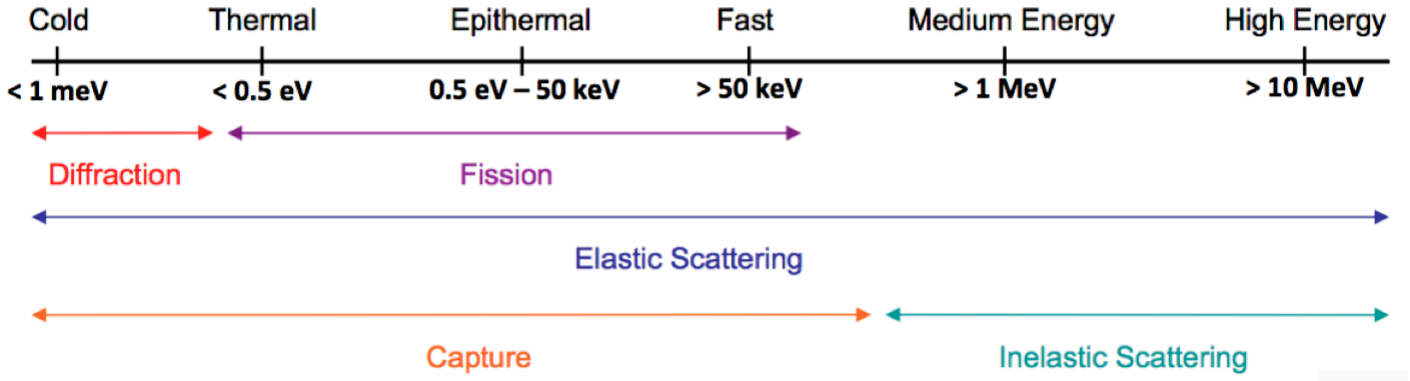

FIGURE 4.11: Classification of free neutrons with the most probable type of interaction with matter.

Neutrons

Fission

The neutron-induced fission occurs at relatively low energies. The target nucleus is split into two or more smaller nuclei and releases a large amount of energy in the form of a secondary emission of neutrons, photons or other types of radiations. This leads to the concept of neutron multiplication and chain reactions used in the nuclear reactors.

Elastic Scattering

The elastic neutron-nucleus scattering $A(n,n)A$ is mainly responsible of the slowing down of the incident neutron, also called the neutron moderation. In this case, the energy and the direction of the neutron are altered and the target nucleus recoils and stays in its ground state. The neutron moderation is the dominant energy loss process from intermediate to high energies.

Neutrons

Neutron Capture

The neutron capture consists of the absorption of the neutron by the medium, followed by the emission of gamma rays in case of a radiative capture (n, γ) or the emission of charged particles such as protons (n, p) or alpha particles (n, α).

Inelastic Scattering

At energies higher than several MeV, the neutrons interact via inelastic scattering $A(n, n')A^*$ with the medium. The neutrons lose a large fraction of their energy and leave the target nuclei in an excited state. Secondary radiations are then emitted from the nuclei when returning to the ground state.

CMS Environment

Simulated BKG and Sensitivities

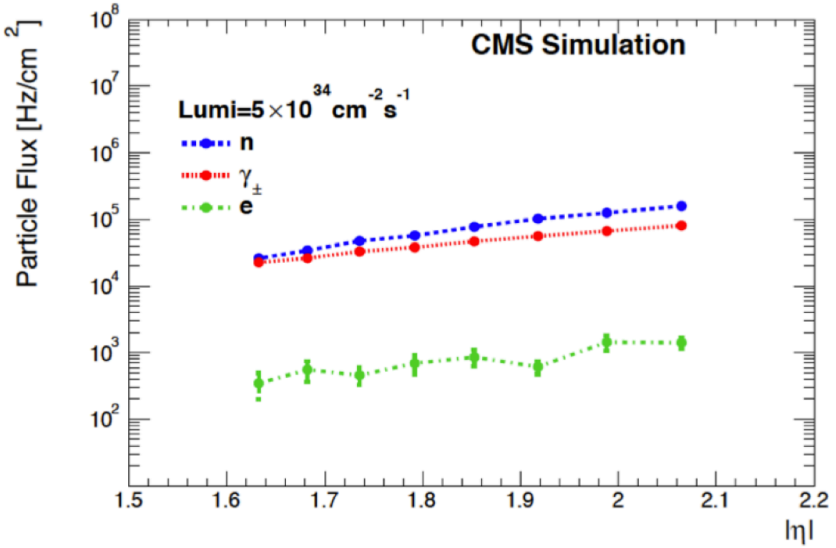

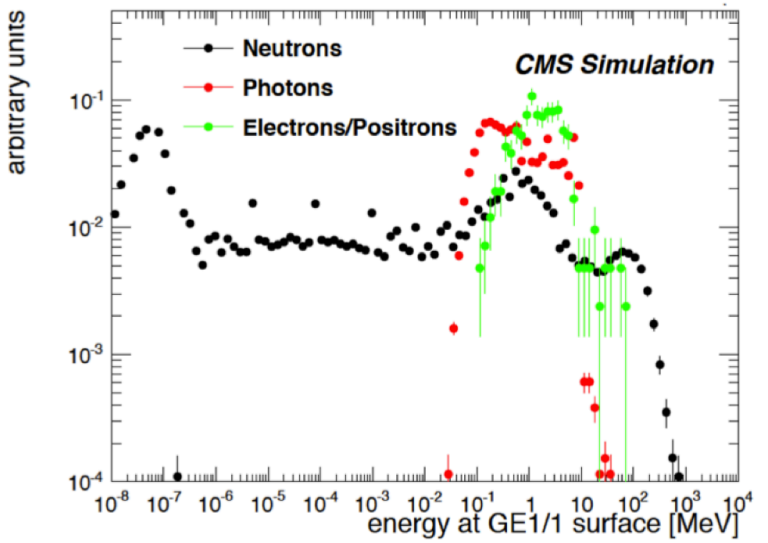

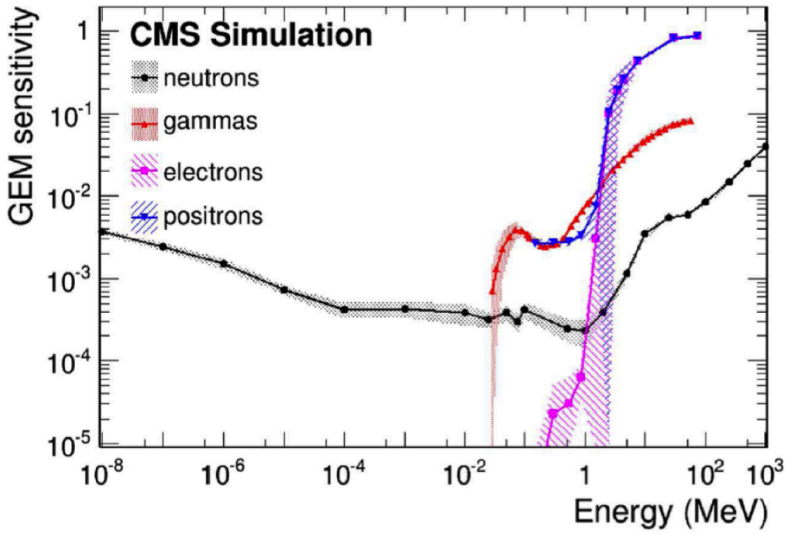

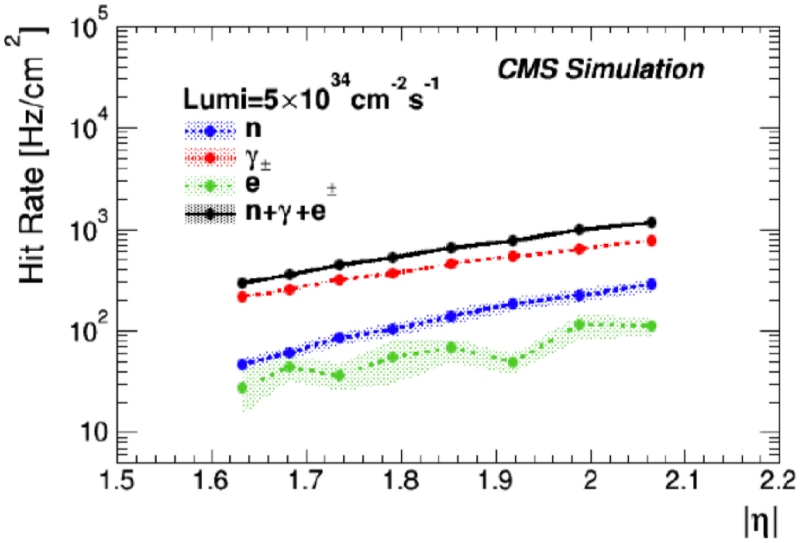

The end


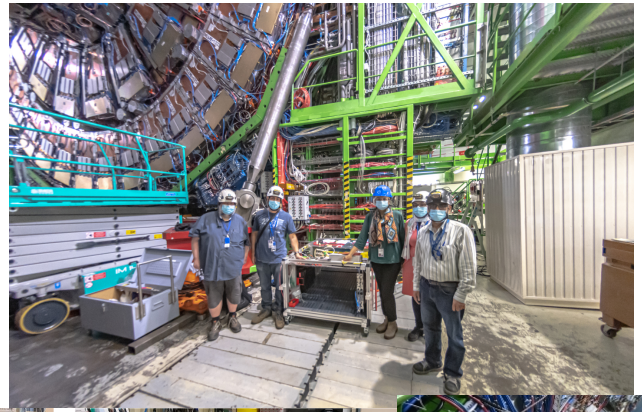



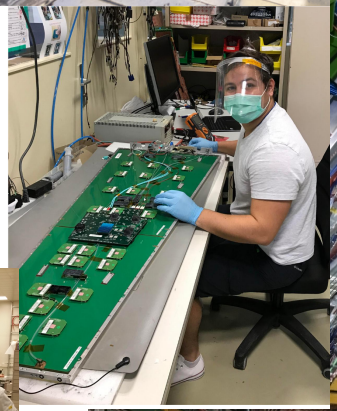

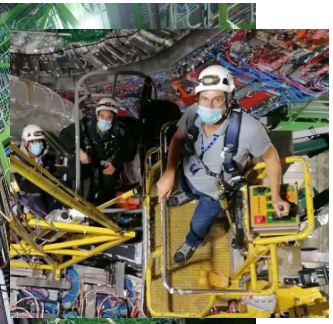

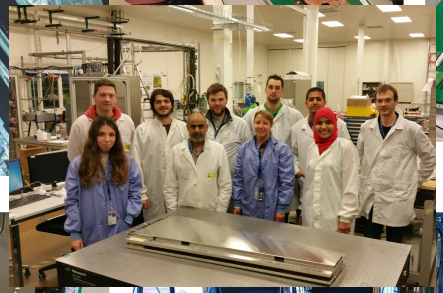

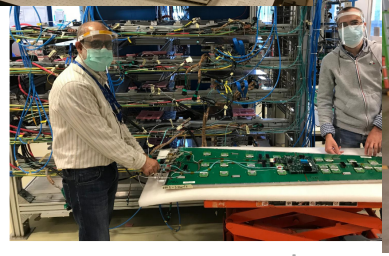


The end


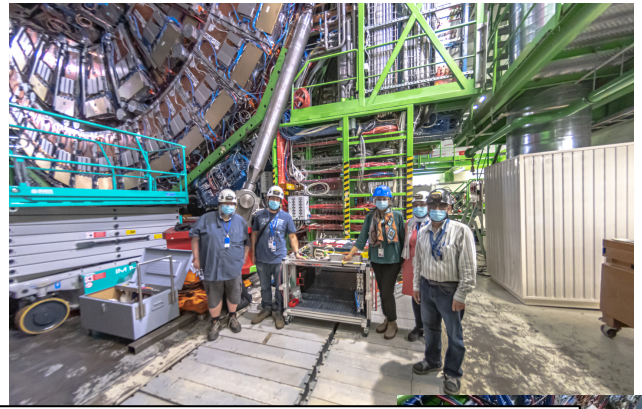




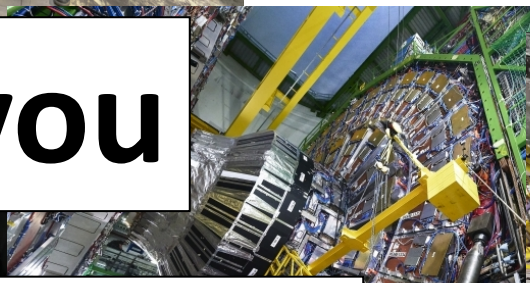




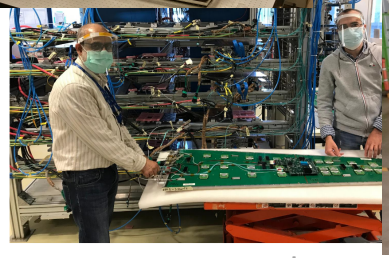

Thank you

Any Questions ?